Acadlore Transactions on Applied Mathematics and Statistics
https://www.acadlore.com/journals/ATAMS

Risk Spillovers and Hedging in the Chinese Stock Market: An Asymmetric VAR-BEKK-AGARCH Analysis

Jia Wang[1,2*], Xun Huang[1], Xu Wang[3]

[1] School of Economics, Northeastern University at Qinhuangdao, 066004 Qinhuangdao, China
[2] College of Business Administration, Northeastern University, 110819 Shenyang, China
[3] School of Economics and Management, Hebei University of Environmental Engineering, 066102 Qinhuangdao, China

* Correspondence: Jia Wang (wangjia@neuq.edu.cn)

Received: 10-15-2023 **Revised:** 11-10-2023 **Accepted:** 11-18-2023

Citation: J. Wang, X. Huang, X. Wang, "Risk spillovers and hedging in the Chinese stock market: An asymmetric VAR-BEKK-AGARCH analysis," *Acadlore Trans. Appl Math. Stat.*, vol. 1, no. 3, pp. 111–129, 2023. https://doi.org/10.56578/atams010301.

Abstract: In the present investigation, the phenomena of multi-scale volatility spillovers and dynamic hedging within the Chinese stock market are scrutinized, with particular emphasis on the implications of structural breaks. The decomposition of the returns from the CSI 300 and Hang sheng index' spot and futures is achieved through the application of the Maximum Overlap Discrete Wavelet Transform (MODWT), categorizing the data into three distinct temporal scales: short-term, medium-term, and long-term. An enhancement upon the conventional VAR-BEKK-GARCH (Vector Autoregressive - Baba, Engle, Kraft, and Kroner - Generalized Autoregressive Conditional Heteroskedasticity) model is proposed, yielding the asymmetric VAR-BEKK-GARCH Model (VAR-BEKK-AGARCH), which adeptly integrates the structural break of return volatility. A comprehensive analysis is conducted to elucidate the interactions and spillovers between the CSI 300 and Hang Seng Index, as well as their respective spot and futures markets, across the various identified time scales. Concurrently, a dynamic hedging portfolio, comprised of index spot and futures, is meticulously constructed, with its performance rigorously evaluated under the influence of the different time scales. To ensure the robustness and validity of the findings, wavelet coherence and phase difference methodologies are employed as verification tools. The results unequivocally reveal a heterogeneity in the behavior of mean spillover, volatility spillover, and asymmetric spillovers between the spot and futures markets of the CSI 300 and Hang Seng Index across the diverse scales. The inclusion of a structural break in the dynamic hedge portfolio is demonstrated to confer a marked advantage over its counterpart that omits this critical factor. Particularly in the short and medium-term scenarios, the dynamically hedged portfolio, enriched by the consideration of the structural break, exhibits superior performance in comparison to the static hedge portfolio. Additionally, it is discerned that the CSI 300 Index and Hang Seng Index, along with their spot and futures components, predominantly manifest in synchrony, with no clear indication of a consistent leader-lag relationship. An intensification of correlation is observed in the long-term analysis, underscoring the utility of the spot and futures of the two indices as efficacious hedging tools.

Keywords: Structural break; Risk spillover; Dynamic hedging; Wavelet coherence

1 Introduction

The futures market, serving as a fundamental component of the financial landscape, plays a crucial role in the elucidation of price mechanisms and the mitigation of financial risks. As the pace of global economic integration quickens, the synergy among financial markets has grown more marked, capturing the attention of scholars around the world. These academics have focused their research on the intricacies of price transmissions, the dynamics of risk spillover, and the complexities of hedging strategies bridging futures and spot markets [1–3]. Precise discernment of the risk transference effects and the channels through which information is conveyed between these two market types is of paramount importance. It equips both individual and institutional investors with the tools required to devise efficacious hedging strategies, refine the accuracy of their investment choices, and effectively reduce the risks associated with decision-making [4].

The utilization of GARCH-type models has been predominant in scholarly research for investigating issues related to risk spillover between markets [5–7]. Pan et al. [8] ingeniously integrated the concept of information spillover from markets into the conventional GARCH framework, synergizing this model with the Chicago Board Options Exchange (CBOE) Volatility Index (VIX) to enhance the forecasting of volatility. In a similar vein, Malik et al. [9] employed the BEKK-GARCH model to meticulously analyze the inter-market volatility spillovers amongst the stock markets of the BRICS nations amidst the tumultuous period of the COVID-19 outbreak. Their findings underscored the model's proficiency in capturing the nuanced dynamics of volatility spillovers between these markets. Dhaene et al. [10] innovatively introduced Sparse Dynamic Conditional Correlation (DCC)-GARCH and Sparse BEKK-GARCH models, applying them to scrutinize the interplay of volatility spillovers and correlations across the 24 constituents of the Bloomberg Commodity Index. Their research illuminated notable spillover effects emanating from the metal and energy markets, subsequently impacting the agricultural market. The susceptibility of financial market volatility to structural breaks necessitates careful consideration, as overlooking these pivotal shifts in market dynamics may result in inaccuracies in the estimation of model parameters, as well as potential misinterpretations of risk spillover across markets [11, 12]. Malik [13] has pioneered the integration of structural breaks into the BEKK-GARCH model, with the specific aim of forecasting volatility patterns in the U.S. financial markets. The empirical results underscore the significance of accounting for structural breaks, revealing a marked reduction in the volatility spillover effects across major U.S. industry markets, and concurrently yielding substantial savings in portfolio management costs. Furthermore, scholarly discourse underscores the merit of amalgamating the study of risk spillover dynamics and hedging intricacies. This synergistic approach not only deepens investors' comprehension of the intricate mechanisms governing cross-market risk transmission but also aids in the strategic assembly of judicious hedging portfolios. Ultimately, the precision in gauging risk spillover effects stands as a catalyst for augmenting portfolio yields and optimizing hedging efficacy [14]. Sarwar et al. [15] engaged a suite of models - BEKK-GARCH, DCC-GARCH, DCC-GARCH, and GO-GARCH - to meticulously scrutinize the volatility spillovers and hedging relationships between the equity markets of the leading three Asian oil-importing nations and the crude oil market. Concurrently, Wen et al. [16] harnessed the capabilities of a time-varying VAR model, delving into the intricate dynamics of risk spillover and associated hedging challenges between the Chinese equity market and the commodity futures market. Their analysis culminated in the insight that a strategically crafted hedging portfolio, comprising grain futures and the Shanghai Composite Index, substantially mitigates portfolio risk. Traditional volatility models predominantly operate under the assumption that positive and negative price shocks exert symmetric effects on conditional variance. However, it is observed in financial markets that negative shocks frequently yield a disproportionately larger impact on conditional variance compared to positive shocks [17]. To encapsulate the asymmetric influences of adverse and favorable news on return volatility, this study incorporates the disparate characteristics of positive and negative shocks into the conventional VAR-BEKK-GARCH framework. This leads to the formulation of an asymmetric VAR-BEKK-GARCH model, termed VAR-BEKK-AGARCH, which additionally accommodates structural breaks in return volatility. The investigation is directed towards elucidating the dynamics of risk spillover and hedging practices between the spot and futures markets of both the CSI 300 and the Hang Seng Index.

The dependency structure between financial markets is intricately linked to the temporal scale, with the correlation and risk spillover effects between markets potentially varying across different time frequencies [18, 19]. A considerable number of scholarly works, predominantly employing wavelet theory, has been conducted to explore the risk spillover and hedging issues across financial markets at varying temporal scales [20]. Wavelet theory, recognized as an exceptionally effective non-linear time series analysis tool, utilizes multi-resolution analysis to decompose original data into multiple sets across different frequencies. This theory has found extensive application in domains such as financial risk and forecasting [21]. Gürbüz and Şahbaz [22], have utilized Discrete Wavelet Transform (DWT) techniques to decompose financial market return series, substantiating the presence of marked disparities in volatility spillover effects between the Turkish futures and spot markets across different time scales. Belhassine and Karamti [23] developed a wavelet-based MGARCH model to examine the volatility spillover effects and hedging between the stock markets of oil-importing and oil-exporting countries across various temporal dimensions. Their findings underscore a clear time-scale dependency in market volatility spillover and hedging strategies. In a similar vein, Zhang et al. [24] employed a wavelet-based BEKK-GARCH-X model to investigate the volatility spillover among the Chinese oil market, renewable energy market, and high-tech market across different time scales. Their results advocate for the consideration of varying time frequencies in the design of differentiated investment portfolios and risk management strategies.

Building upon the foundation of prior research, this manuscript introduces the asymmetric VAR-BEKK-AGARCH model, incorporating structural breaks to investigate the multi-scale risk spillover and dynamic hedging issues between the spot and futures markets of the CSI 300 and Hang Seng Index. Three primary contributions are delineated:

Firstly, the Maximal Overlap Discrete Wavelet Transform (MODWT) is employed to decompose the spot and

futures of the CSI 300 and Hang Seng Index into short-term, medium-term, and long-term returns series at various temporal scales.

Secondly, the asymmetric effects of positive and negative shocks are integrated into the traditional VAR-BEKK-GARCH framework, leading to the development of the asymmetric VAR-BEKK-AGARCH model. This model takes into account the structural breaks in return volatility, enabling the analysis of mean spillover, volatility spillover, and asymmetric spillover effects between the CSI 300 and Hang Seng Index, as well as between their respective spot and futures markets across different time scales. Concurrently, dynamic hedging portfolios between the index spot and futures are constructed. The performance of these hedging portfolios, considering structural breaks, is then contrasted with the performance of hedging portfolios that do not take structural breaks into account, as well as with static hedging portfolios.

Thirdly, the empirical results are validated through the use of wavelet coherence and phase difference, exploring the correlation and lead-lag relationships between markets in the time-frequency domain. This approach ensures that the findings are both comprehensive and robust.

2 Model and Methodology

2.1 MODWT

Wavelet transform, based on the theoretical framework of Fourier transform, serves as a nonlinear time series analysis tool that decomposes original signals into various frequency domains through dilation and translation operations. The MODWT is an enhancement of the DWT, overcoming the limitations of DWT with regard to sample size and possessing translation invariance, thus maintaining signal length consistency after each decomposition. In this study, the MODWT is utilized to decompose the return series of both spot and futures for the CSI 300 and Hang Seng Index into a series of sub-sequences at different frequencies.

Two types of MODWT filters, namely the wavelet filter $\left\{\tilde{h}_l \mid l=0,\ldots,L_j\right\}$ and scale filter $\{\tilde{g}_l \mid l=0,\ldots,L_j\}$, are considered for the cyclic filtration decomposition of the original series $X_t(t=1,2,\cdots,T)$, wherein $j=1,\cdots,J$ and J are scale parameters, and J represents the maximum scale of the decomposed X_t, the wavelet coefficient and scale coefficient at the j-th level of decomposition are represented as $\widetilde{W}_{j,t}$ and $\widetilde{V}_{j,t}$, respectively:

$$\widetilde{W}_{j,t}=\sum_{l=0}^{L_j-1}\tilde{h}_{j,l}X_{t-l},\quad \widetilde{V}_{j,t}=\sum_{l=0}^{L_j-1}\tilde{g}_{j,l}X_{t-l} \tag{1}$$

where, the wavelet filter $\tilde{h}_{j,l}$ satisfies the constraints $\sum_{l=0}^{L_j-1}\tilde{h}_{j,l}=0$, $\sum_{l=0}^{L_j-1}\tilde{h}_{j,l}^2=2^{-j}$ and $\sum_{l=-\infty}^{\infty}\tilde{h}_{j,l}\tilde{h}_{j,l+2^jn}=0$, whereas the scale filter meets the constraints $\sum_{l=0}^{L_j-1}\tilde{g}_{j,l}=1$, $\sum_{l=0}^{L_j-1}\tilde{g}_{j,l}^2=2^{-j}$, $\sum_{l=-\infty}^{\infty}\tilde{g}_{j,l}\tilde{g}_{j,l+2^jn}=0$ and $\sum_{l=-\infty}^{\infty}\tilde{g}_{j,l}\tilde{h}_{j,l+2^jn}=0$. The length of the wavelet coefficient $\widetilde{W}_{j,t}$ is equivalent to that of X_t. According to Eq. (1), the original series X_t can be obtained through the j-th level details $\widetilde{D}_{j,t}=\sum_{l=0}^{L_j-1}\tilde{h}_{j,l}\widetilde{W}_{j,t+l}$ of MODWT and the J-th level smoothness or approximation of $\widetilde{S}_{J,t}=\sum_{l=0}^{L_J-1}\tilde{g}_{J,l}\widetilde{V}_{J,t+l}$.

Finally, the original time series X_t is reconstructed from the detail part $\widetilde{D}_{j,t}$ and the approximated part $\tilde{S}_{j,t}$, as expressed in Eq. (2).

$$X_t=\sum_{j=1}^{J}\widetilde{D}_{j,t}+\widetilde{S}_{J,t} \tag{2}$$

2.2 Structural Break Detection Based on the Modified Iterative Cumulative Sum of Squares (ICSS)

Existing research has demonstrated that volatility structures in financial markets exhibit characteristics of structural breaks, which can significantly influence the dependency structures and risk spillover between markets [25]. Therefore, when the time span of the sample under study is substantial, it becomes necessary to detect structural breaks in market volatility to reduce the estimation risk of the model. In this study, the modified ICSS algorithm [26, 27] is employed to identify structural break points in the volatility of the CSI 300 and Hang Seng Index spot and futures markets across different scales.

The ICSS algorithm, proposed by Inclan and Tiao, assumes that the variance of the return series is initially stable but undergoes a change due to the impact of sudden events, after which it remains stable until the occurrence of the next break. The positions where variance changes are identified as structural break points. The specific process is outlined as follows:

Let $\varepsilon_t\sim N\left(0,\sigma_t^2\right)$ denote the return residuals series, and $t=1,2,\cdots,T$; where N_T is the number of structural breaks in a series of T observations. The return series is divided into N_T+1 intervals, with the sequence of structural

break points represented as $\{k_1, k_2, \ldots, k_{N_T}\}, 1 < k_1 < k_2 < \ldots < k_{N_T} < T$. The variances of these intervals are denoted as τ_j^2, $j = 0, 1, \ldots, N_T$, then there are:

$$\sigma_0^2 = \begin{cases} \tau_0^2, 1 < t < k_1 \\ \tau_1^2, k_1 < t < k_2 \\ \ldots \\ \tau_{N_T}^2, k_{N_T} < t < T \end{cases} \tag{3}$$

Then, the cumulative sum of squared residuals up to time m is defined as $C_k = \sum_{t=1}^{m} \varepsilon_t^2, (m = 1, 2, \cdots, T)$, and the test statistic is $IT = \sup_m \left| D_m \sqrt{T/2} \right|$, where $D_m = \frac{C_m}{C_T} - \frac{m}{T}$, $D_0 = D_T = 0$. If there are no structural breaks in variance up to time m, then D_m will oscillate around zero; if there are structural break points, then D_m will significantly deviate from zero. Let m^* be the value of m when $\max_m |D_m|$ is attained. If $\max_m \left| D_m \sqrt{T/2} \right|$ exceeds a predetermined critical value, then m^* is considered a variance break point, where $\sqrt{T/2}$ is a standardization factor.

The test statistic IT in the ICSS algorithm is calculated under the assumption that the return residual follows the normal distribution. However, return series in financial markets often exhibit leptokurtic and heavy-tailed characteristics. Therefore, the use of the IT statistic to detect structural breaks in return volatility can often lead to failures. To address this issue, a modified test statistic is proposed and represented as [26]:

$$\widetilde{IT} = \sup_m \left| G_m T^{-1/2} \right| \tag{4}$$

where, $G_m = \left(C_m - \frac{m}{T} C_T\right) / \sqrt{\hat{\omega}}$, $\hat{\omega}$ is a non-parametric estimator of ω, $\hat{\omega} = \frac{1}{T} \sum_{t=1}^{T} \left(\varepsilon_t^2 - \hat{\sigma}^2\right)^2 + \frac{2}{T} \sum_{\xi=1}^{\Gamma} w(\xi, \Gamma), \sum_{t=\xi+1}^{T} \left(\varepsilon_t^2 - \hat{\sigma}^2\right) \left(\varepsilon_{t-\xi}^2 - \hat{\sigma}^2\right), \hat{\sigma}^2 = C_T/T$, $w(\xi, \Gamma) = 1 - \xi/(\Gamma + 1)$ and Γ is the Bartlett Kernel bandwidth.

2.3 The VAR-BEKK-AGARCH Model with Structural Breaks Taken into Consideration

With the asymmetry of positive and negative shocks taken into consideration, an asymmetric VAR-BEKK-GARCH (VAR-BEKK-AGARCH) model was constructed. Additionally, volatility structural breaks were incorporated to investigate mean spillover, volatility spillover, and asymmetric spillover effects across various markets at different time scales.

(1) Mean Equation VAR(1)

The VAR model was utilized to represent the mean equation, expressed as:

$$\mathbf{Y}_t(j) = \varphi + \phi \mathbf{Y}_{t-1}(j) + \varepsilon_t(j), \varepsilon_t = \sqrt{h_t} z_t z_t \sim iid \tag{5}$$

where, $\mathbf{Y}_t(j)$ is a (2×1) vector, representing the j-th level wavelet details of the return series at time t; φ is a (2×1) vector of constants; $\phi = [\phi_{11}\phi_{12}; \phi_{21}\phi_{22}]$ is a (2×2) matrix of first-order autoregressive coefficients, with diagonal elements and representing the impact of market 1 (market 2) on its own first-order lag, and off-diagonal elements ϕ_{12} (ϕ_{21}) representing the mean spillover effects from variable 1 (variable 2) to variable 2 (variable 1). $\varepsilon_t(j)$ is a vector of independently and identically distributed random errors at time t on wavelet scale j, assumed to follow the Student-t distribution [28].

(2) Variance Equation

In the traditional BEKK-GARCH model, the impact of positive and negative price shocks on conditional variance is symmetric, failing to explain the asymmetric impact of bad and good news on return volatility. This article considers the asymmetry of positive and negative shocks and constructs an asymmetric VAR-BEKK-GARCH (VAR-BEKK-AGARCH) model. Furthermore, structural breaks in return volatility are considered, and detected structural break points are introduced as dummy variables into the VAR-BEKK-AGARCH model. The variance equation is expressed as follows:

$$H_t(j) = C'C + A'\varepsilon_{t-1}(j)\varepsilon'_{t-1}(j)A + B'H_{t-1}(j)B + G'\eta_{t-1}(j)\eta'_{t-1}(j)G + \sum_{i=1}^{q} d'_i D'_i(j) D_i(j) d_i \tag{6}$$

$$H_t(j) = \begin{pmatrix} h_{11,t}(j) & h_{12,t}(j) \\ h_{21,t}(j) & h_{22,t}(j) \end{pmatrix} \tag{7}$$

$$C = \begin{pmatrix} c_{11} & 0 \\ c_{21} & c_{22} \end{pmatrix} A = \begin{pmatrix} a_{11} & a_{12} \\ a_{21} & a_{22} \end{pmatrix} B = \begin{pmatrix} b_{11} & b_{12} \\ b_{21} & b_{22} \end{pmatrix} G = \begin{pmatrix} g_{11} & g_{12} \\ g_{21} & g_{22} \end{pmatrix} \tag{8}$$

where, C is a (2×2) lower triangular matrix of constant coefficients; A, B, and G are (2×2) coefficient matrices. Matrix A measures the impact of random shocks on volatility, representing ARCH-type volatility spillover. Matrix B measures the impact of past conditional variance on current volatility, representing GARCH-type volatility spillover. The diagonal elements a_{11} (a_{22}) and b_{11} (b_{22}) of matrices A and B respectively represent the impact of the previous period's volatility of variable 1 (variable 2) on its current volatility; and off-diagonal elements a_{12} (a_{21}) and b_{12} (b_{21}) respectively represent the ARCH and GARCH volatility spillover effects from variable 1 (variable 2) to variable 2 (variable 1). Matrix G measures the asymmetric response of conditional variance to negative shocks; if ε_t is negative, then $\eta_t = \varepsilon_t$; otherwise $\eta_t = 0$. The diagonal elements g_{11} (g_{22}) represent the asymmetric impact of previous period's volatility of variable 1 (variable 2) on its current volatility; the off-diagonal elements g_{12} (g_{21}) represent the asymmetric spillover effects from variable 1 (variable 2) to variable 2 (variable 1). D_i is a (1×2) dummy variable matrix, describing the structural breaks in variances; d_i is a (2×2) lower triangular matrix of constant coefficients; q represents the quantity of structural breaks.

2.4 Dynamic Hedging Model

Assuming that at time t, the investor holds a long position of one unit in the spot of the CSI 300 Index or the Hang Seng Index, and simultaneously holds a short position of β_t units in the index futures to hedge risk. The hedge ratio was estimated using the minimum variance method. The smaller the variance σ_p^2 of the investment portfolio, the more optimal the hedging strategy, with the objective function being:

$$\min \sigma_p^2(j) = \min \left[\mathrm{var}\left(R_{s,t}(j) - \beta_t(j) R_{f,t}(j)\right)\right] = h_{ss,t}(j) + \beta_t^2(j) h_{ff,t}(j) - 2\beta_t(j) h_{sf,t}(j) \tag{9}$$

where, $\beta_t(j)$ represents the hedge ratio at time t under the j-th level scale, $R_{s,t}(j)$ and $R_{f,t}(j)$ respectively denote the spot and futures returns under the the j-th level scale, while $h_{ss,t}(j)$ and $h_{ff,t}(j)$ represent the variances of spot and futures returns under the j-th level scale, respectively. Consequently, the optimal hedge ratio for the spot and futures under the j-th level scale was determined to be:

$$\beta_t(j) = \frac{h_{sf,t}(j)}{h_{ff,t}(j)} \tag{10}$$

To analyze the effectiveness of the hedging, the Hedge Effectiveness (HE) ratio was introduced, quantified by the equation:

$$\mathrm{HE}_t(j) = \frac{V_t^{uhg}(j) - V_t^{hg}(j)}{V_t^{uhg}(j)} \tag{11}$$

where, $V_t^{uhg}(j)$ is the variance of the spot without hedging at time t under the j-th level scale, and $V_t^{hg}(j)$ is the variance of the hedged portfolio at time t under the j-th level scale. $\mathrm{HE}_t(j)$ represents the risk reduction ratio at time t under the j-th level scale, the closer its value is to 1, the greater the extent to which the portfolio risk is reduced after hedging, indicating a more effective hedging strategy.

2.5 Wavelet Coherence and Phase Difference

Wavelet coherence can be regarded as the local correlation of two time series, X_t and Y_t, in the time-frequency domain [29]. Assuming the mother wavelet is ψ, various daughter wavelets $\psi_{s,\lambda}$ are generated through scaling and translation, represented as:

$$\psi_{s,\lambda} = \frac{1}{\sqrt{|s|}} \psi\left(\frac{t-\lambda}{s}\right), s, \lambda \in \mathbb{R} \tag{12}$$

where, s and λ denote the scale and location parameters. The Continuous Wavelet Transform (CWT) of a time series $X_t \in L^2(\mathbb{R})$ is defined as:

$$W_X(s,\lambda) = \langle X, \psi_{s,\lambda} \rangle = \int_{-\infty}^{+\infty} X_t \frac{1}{\sqrt{|s|}} \psi^*\left(\frac{t-\lambda}{s}\right) dt \tag{13}$$

where, $L^2(\mathbb{R})$ denotes the Hilbert space of square-integrable functions, and $*$ represents the complex conjugate. The time-scale distribution of time series X_t is obtained by adjusting s and λ.

The wavelet coherence of two time series X_t and Y_t can be expressed as:

$$R_{XY}^2(s,\lambda) = \frac{\left| S\left(s^{-1} W_{XY}(s,\lambda)\right)\right|^2}{S\left(s^{-1}\left|W_X(s,\lambda)\right|^2\right) S\left(s^{-1}\left|W_Y(s,\lambda)\right|^2\right)} \tag{14}$$

where, S is a smoothing factor with respect to time and scale, $W_{XY}(s,\lambda) = W_X(s,\lambda)W_Y^*(s,\lambda)$ represents the cross wavelet transform, and $|W_{XY}(s,\lambda)|$ denotes the cross wavelet power spectrum. $R^2_{XY}(s,\lambda)$ measures the cross-correlation of X_t and Y_t in the time-frequency domain, and $0 \leq R^2_{XT}(s,\lambda) \leq 1$.

While wavelet coherence measures the positive correlation between two time series at different scales, it does not capture their negative correlation or provide phase information. Phase difference reveals the details of the oscillation cycles between two correlated time series, indicating their lead-lag relationship [29]. Introducing phase difference on the basis of wavelet coherence allows for the measurement of both positive and negative correlations between two time series, as well as their lead-lag relationship at different scales. The phase difference in wavelet coherence is expressed as:

$$\phi_{XY}(s,\lambda) = \tan^{-1}\left(\frac{\mathrm{Im}\left\{W_{XY}(s,\lambda)\right\}}{\mathrm{Re}\left\{W_{XY}(s,\lambda)\right\}}\right), \phi_{XY}(s,\lambda) \in [-\pi,\pi] \tag{15}$$

where, *Im* and *Re* respectively represent the imaginary and real parts of the cross wavelet transform. $\phi_{XI}(s,\lambda)$ describes the phase difference between the components of X_t and Y_t at various scales. The direction of arrows in the wavelet coherence plot is utilized to interpret the phase difference. Arrows pointing right (left) indicate X_t and Y_t are in same phase (opposite phase). When arrows point directly upwards or downwards, no conclusion can be drawn. Arrows pointing to the top-right or bottom-left indicate that X_t leads Y_t, while arrows pointing to the top-left or bottom-right suggest that Y_t leads X_t. In this study, wavelet coherence and phase difference were employed to assess the time-frequency correlation and lead-lag relationship between two time series.

3 Empirical Analysis

In this section, the MODWT method described in Section 1.1 was employed to perform wavelet decomposition on the return series of the CSI 300 and Hang Seng Index futures and spot prices at short-term, medium-term, and long-term time scales. Subsequently, the VAR-BEKK-AGARCH model incorporating structural breaks, constructed in Section 1.3, was utilized to estimate the mean spillover, volatility spillover, and asymmetric spillover effects of the returns of the CSI 300 and Hang Seng Index. The hedging performance of minimum risk between the spot and futures of each index was also analyzed. Finally, the wavelet coherence and phase difference methods were applied to validate the robustness of the empirical results.

3.1 Data

The sample consists of spot and futures price data for the CSI 300 and Hang Seng Index, spanning from January 4, 2013, to June 2, 2022, resulting in 2222 trading days after excluding days that differ due to market holidays. The spot prices are represented by the daily closing prices, while the futures prices are represented by the daily settlement prices. All data were sourced from the Wind database. The market return rate is denoted by $r_t = (\ln(P_t) - \ln(P_{t-1})) \times 100$, where P_t is the closing or settlement price on day t. Figure 1 presents the return trends of the spot and futures for the CSI 300 (denoted as CSI300) and Hang Seng Index (denoted as HSI). It can be observed from Figure 1 that the returns of both the spot and futures of each index exhibit characteristics of volatility clustering. When studying the risk spillover effects between markets, it is necessary to introduce structural breaks to fit the volatility characteristics of the index returns.

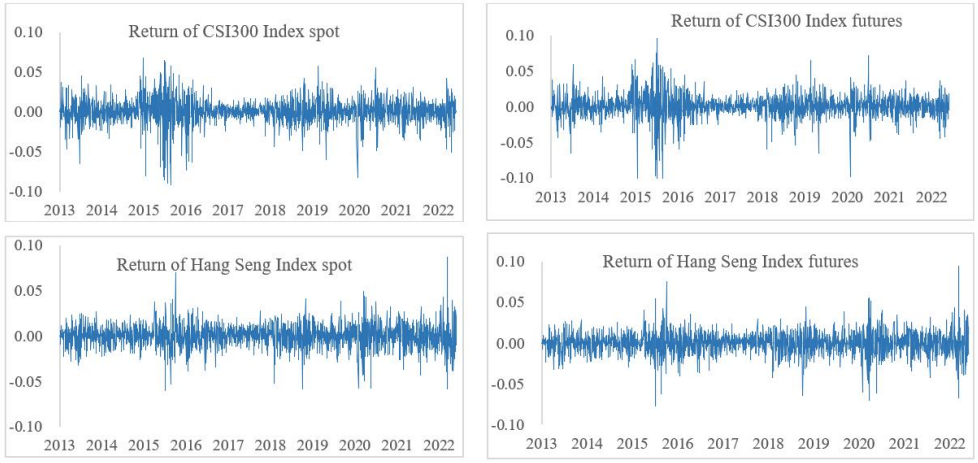

Figure 1. Series of return rates for CSI 300 and Hang Seng Index futures and spot

3.2 Analysis of Wavelet Decomposition Results

Wavelet decomposition has been performed on the return series of the spot and futures of the CSI 300 and Hang Seng Index. Referring to the study [30] for the selection of a wavelet scale J=5. The results are depicted in Figures 2–5, with d_1-d_5 representing the detail components at each level, where the frequency decreases progressively. The approximation component is denoted as a_5, and s represents the original signal series. Table 1 details the time scales corresponding to each wavelet detail. Descriptive statistics for the wavelet details of the returns of the spot and futures for each index are provided in Table 2.

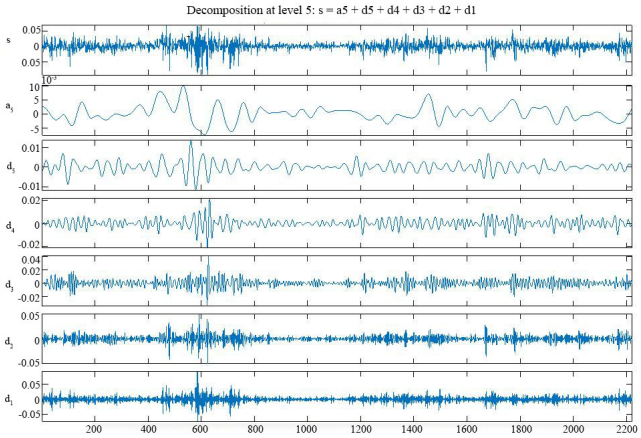

Figure 2. Wavelet decomposition of logarithmic returns for CSI 300 Index spot

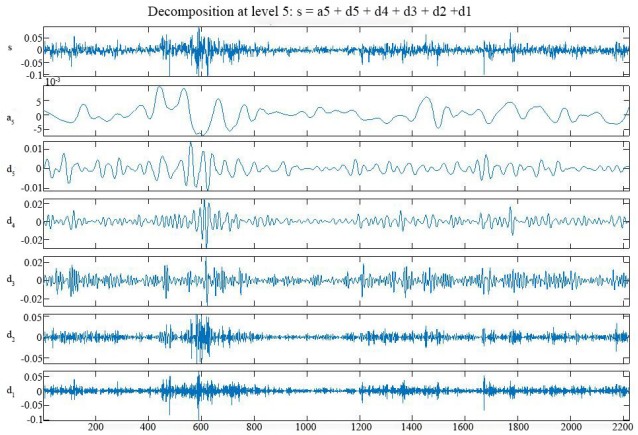

Figure 3. Wavelet decomposition of logarithmic returns for CSI 300 Index futures

Table 1. Time scales corresponding to wavelet details

Wavelet Decomposition Scale	Time Scale (days)	Scale
d_1	$2-4$	Short-term
d_2	$4-8$	Medium-term
d_3	$8-16$	
d_4	$16-32$	Long-term
d_5	$32-64$	

From the perspective of time-domain analysis, (1) it can be observed from Figures 2 and 3 that the high-frequency fluctuations of the CSI 300 index predominantly occur at observation points 590-800, 1360-1500, and 2100-2200. The corresponding time intervals are July 8, 2015, to May 25, 2016; September 28, 2018, to May 14, 2019; and November 23, 2021, to May 31, 2022. These intervals coincide with three major events: the Chinese stock market crash, global trade frictions, and the Russo-Ukrainian War. (2) As depicted in Figures 4 and 5, the high-frequency

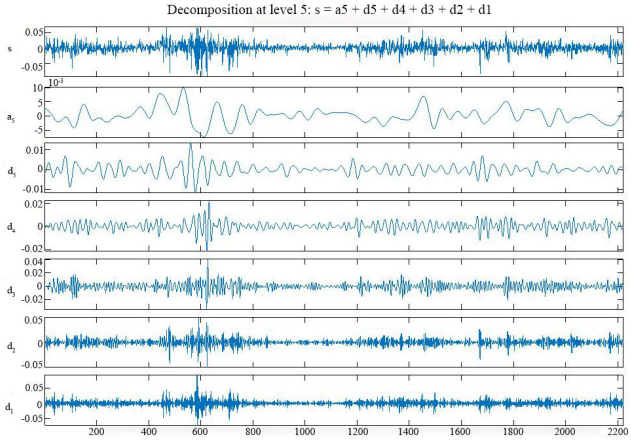

Figure 4. Wavelet decomposition of logarithmic returns for Hang Seng Index spot

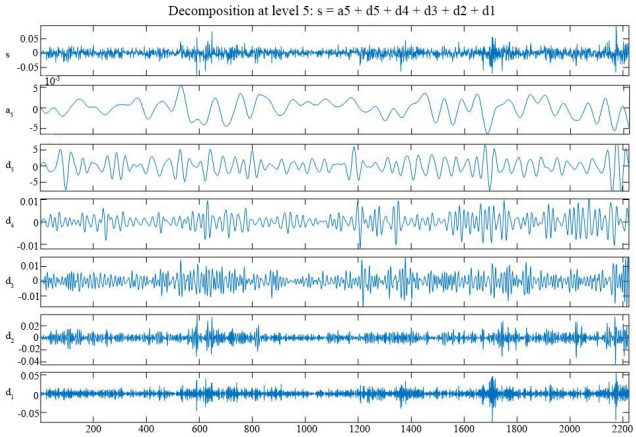

Figure 5. Wavelet decomposition of logarithmic returns for Hang Seng Index futures

fluctuations of the Hang Seng Index mainly occur at observation points 590-700, 1350-1450, and 2100-2200, between January 4, 2013, and June 2, 2022. The corresponding time intervals are July 8, 2015, to December 22, 2015; September 13, 2018, to February 22, 2019; and November 23, 2021, to May 31, 2022. The intervals and events are similar to those of the CSI 300. It can be deduced that there is a significant correlation between the two markets, and their volatilities are alike, although the Shanghai and Shenzhen markets are influenced by financial events for a longer duration.

From the perspective of frequency-domain analysis, as illustrated in Figures 2–5 and Table 1, (1) d_1 describes short-term market fluctuations, with dense high-frequency fluctuations in both the CSI 300 and Hang Seng markets. (2) d_2 and d_3 depict mid-term market fluctuations, manifesting as large shock effects from major sudden events and the market's continuous adjustment process post these events. Both markets exhibit characteristics of significant volatility at certain points and sustained minor fluctuations. (3) d_4 and d_5 describe long-term market fluctuations, with both markets showing the impact of major sudden events on the market, while minor fluctuations are filtered out. The decomposition results from the time-frequency domain reveal significant correlations between the CSI 300 and Hang Seng Index, as well as between the spot and futures of the same index.

Table 2 reveals that (1) the mean of the return rates for each market is close to 0, and the standard deviation decreases with lower frequency, indicating smaller amplitude of return fluctuations; (2) the skewness of the return rates at each scale is non-zero, and the kurtosis is greater than 3, suggesting that the return rates at each scale exhibit characteristics of sharp peaks and heavy tails. (3) According to the Augmented Dickey-Fuller (ADF) test results, the series of return rates at each scale are stationary; (4) the Jarque-Bera test results indicate that the series of return rates at each scale do not follow a normal distribution. These results validate the appropriateness of employing the VAR-BEKK-AGARCH model based on the Student-t distribution to fit the volatility characteristics of the returns in this study.

Table 2. Descriptive statistics of wavelet details for index returns

		CSI 300 Spot	CSI 300 Futures	Hang Seng Spot	Hang Seng Futures
d_1	Mean	0.0002	0.0002	0.0000	0.0000
	Standard Deviation	0.0104	0.0114	0.0087	0.0089
	Skewness	−0.0154	−0.0051	−0.1638	−0.2576
	Kurtosis	9.6625	9.7661	6.6981	8.4278
	ADF	−96.4102***	−93.2214***	−96.4102***	−93.2214***
	J − B	2752.1***	1276.1***	4238.5***	4109.7***
d_2	Mean	0.0002	0.0002	0.0000	0.0000
	Standard Deviation	0.0076	0.0079	0.0060	0.0060
	Skewness	−0.1423	0.0981	−0.0601	−0.0260
	Kurtosis	8.2448	16.6556	7.1370	6.9716
	ADF	−32.4337***	−32.2150***	−32.4337***	−32.2150***
	J-B	1460.6***	1585.9***	17268***	2554.3***
d_3	Mean	0.0002	0.0002	0.0000	0.0000
	Standard Deviation	0.0052	0.0057	0.0043	0.0044
	Skewness	0.0710	0.0139	0.0087	0.0175
	Kurtosis	6.8484	7.7386	4.3439	4.2355
	ADF	−14.7201***	−14.8484***	−14.7201***	−14.8484***
	J-B	141.4359***	167.2410***	279.9319***	1373***
d_4	Mean	0.0002	0.0002	0.0000	0.0000
	Standard Deviation	0.0037	0.0039	0.0030	0.0031
	Skewness	−0.1416	0.0200	−0.1081	−0.1009
	Kurtosis	6.5089	13.2774	3.9648	3.8702
	ADF	−7.7450***	−7.7539***	−7.7450***	−7.7539***
	J − B	73.8706***	90.5023***	9779.2***	1147.3***
d_5	Mean	0.0002	0.0002	0.0000	0.0000
	Standard Deviation	0.0027	0.0028	0.0020	0.0020
	Skewness	0.0010	0.0124	−0.0839	−0.0721
	Kurtosis	6.1192	6.0851	4.1339	4.2297
	ADF	−3.8333***	−3.8147***	−3.8333***	−3.8147***
	J − B	141.9146***	121.6405***	881.2332***	900.7953***

Note: *** indicates significance at the 1% level

3.3 Analysis of Risk Spillover Effects

Four sets of return portfolios were considered, including the spot of the CSI 300 Index and the Hang Seng Index, the futures of the CSI 300 Index and the Hang Seng Index, the spot and futures of the CSI 300 Index, and the spot and futures of the Hang Seng Index. A comparison was conducted between the estimation results of the VAR(1)-BEKK-AGARCH(1,1) model, which takes into account structural breaks, and that which does not consider structural breaks, as established in Section 1, see Table 3. It is observed that, at identical time scales, the values of the Log Likelihood Function (LogL) for the VAR(1)-BEKK-AGARCH(1,1) model incorporating structural breaks are higher than those for the model without structural breaks. Furthermore, the Akaike Information Criterion (AIC) values for the former are found to be lower than those for the latter. This indicates that, in comparison to the VAR(1)-BEKK-AGARCH(1,1) model that does not account for structural breaks, the model that does is more applicable to the stock market data in China. Tables 4–7 list the fitting results of the VAR(1)-BEKK-AGARCH(1,1) model, incorporating structural breaks, for the four sets of return data. The test results of structural breaks at different time scales in each market can be found in the appendix.

Table 3. Comparison results of two VAR(1)-BEKK-AGARCH(1,1) models

	Considering Structural Breaks					**Not Considering Structural Breaks**				
	d_1	d_2	d_3	d_4	d_5	d_1	d_2	d_3	d_4	d_5
Spot of the CSI 300 Index and the Hang Seng Index										
log L	16969	18204	22236	29351	36829	16955	18150	22126	28701	35133
AIC	-33896	-36258	-44430	-56661	-69616	-33865	-36241	-44423	-55246	-68111
Futures of the CSI 300 Index and the Hang Seng Index										
log L	16757	17958	22402	28489	34803	16504	17899	22402	28139	34473
AIC	-33358	-35766	-44763	-56841	-67463	-32967	-35756	-44763	-56236	-68905
Spot and futures of the CSI 300 Index										
log L	18772	20231	25100	31726	38938	18701	20185	25049	31675	37190
AIC	-37418	-40337	-50116	-63332	-77744	-37361	-40329	-50056	-63309	-77338
Futures of the Hang Seng Index										
log L	19641	21247	27189	33125	37897	19628	21224	27154	33077	37555
AIC	-39144	-42363	-54301	-66118	-75663	-39015	-42106	-54176	-66002	-73068

Table 4. Estimation results of the VAR(1)-BEKK-AGARCH(1,1) model considering structural breaks (CSI 300 Index spot and Hang Seng Index spot)

	$\mathbf{d_1}$	$\mathbf{d_2}$	$\mathbf{d_3}$	$\mathbf{d_4}$	$\mathbf{d_5}$
Mean Equation					
φ_1	0.0000	0.0000	0.0000	0.0001^{***}	0.0002^{***}
ϕ_{11}	-0.7198^{***}	0.3514^{***}	0.8132^{***}	1.0015^{***}	0.9955^{***}
ϕ_{12}	-0.0010	0.0846^{***}	0.0000	-0.0043	-0.0028^{***}
φ_2	-0.0001^{***}	0.0000	0.0000	0.0000^{***}	0.0000^{**}
ϕ_{21}	-0.0330^{***}	0.0004	-0.0437^{***}	0.0486^{***}	0.0199^{***}
ϕ_{22}	-0.6972^{***}	0.3538^{***}	0.8673^{***}	0.9065^{***}	0.9784^{***}
Variance Equation					
c_{11}	0.0021^{***}	0.0011^{***}	0.0002^{***}	0.0001^{***}	0.0000^{***}
c_{21}	0.0015^{***}	0.0009^{***}	0.0004^{***}	0.0000^{***}	0.0000^{***}
c_{22}	0.0017^{***}	0.0011^{***}	0.0000	0.0000^{***}	0.0000^{***}
a_{11}	0.8425^{***}	0.8971^{***}	1.0670^{***}	1.5145^{***}	1.6132^{***}
a_{12}	0.0401	0.0344	0.0021	-0.0288^{***}	-0.0131^{***}
a_{21}	0.0794^{**}	-0.1224^{***}	0.0126	-0.0167	0.0061^{**}
a_{22}	0.8199^{***}	0.8337^{***}	1.1032^{***}	1.5502^{***}	1.6203^{***}
b_{11}	0.7048^{***}	0.6995^{***}	0.7103^{***}	-0.4510^{***}	0.4530^{***}
b_{12}	-0.0219	-0.0172	0.4846^{***}	0.0088^{***}	-0.0003
b_{21}	-0.0612^{***}	0.0606^{***}	-0.2953^{***}	-0.0031	-0.0001
b_{22}	0.6601^{***}	0.7033^{***}	-0.6321^{***}	-0.4704^{***}	0.4522^{***}
g_{11}	-0.0225	-0.1736	-0.1447	-0.1791^{***}	0.0001
g_{12}	0.1252^{***}	-0.1504^{***}	-0.0166	0.0083	-0.0233^{***}
g_{21}	-0.1144	0.1992^{***}	0.1499^{***}	-0.0306	-0.0016
g_{22}	-0.4855^{***}	-0.2849^{**}	-0.0143	-0.2154^{***}	0.0299

Note: ***, **, and * denote significance levels at 1%, 5%, and 10%. 1 and 2 respectively represent the CSI 300 Index spot and the Hang Seng Index spot, respectively

From Table 4, it can be deduced that in terms of mean spillover effects: (1) ϕ_{11} and ϕ_{22} are significant across all time scales, indicating a substantial impact of the lagged terms of the CSI 300 and Hang Seng Index spot returns on themselves; (2) ϕ_{12} is significant at the d_2 and d_5 scales, suggesting mean spillover effects from the CSI 300 Index spot to the Hang Seng Index spot at these scales. ϕ_{21} is significant across all scales except d_2, indicating short-term and long-term mean spillover effects from the Hang Seng Index spot to the CSI 300 Index spot. In terms of volatility spillover effects: (1) a_{11}, a_{22}, b_{11}, and b_{22} are significant across all time scales, denoting that the volatility of both indices' spot is highly influenced by their own lagged terms; (2) a_{12} is significant at the d_4 and d_5 scales, indicating long-term ARCH spillover effects from the CSI 300 Index spot to the Hang Seng Index spot; a_{21} is significant at the d_1, d_2, and d_5 scales, suggesting ARCH spillover effects from the Hang Seng Index spot to the CSI 300 Index spot across these scales; (3) b_{12} is significant at the d_3 and d_4 scales, indicating GARCH spillover effects from the CSI 300 Index spot to the Hang Seng Index spot at these scales; b_{21} is significant at the d_1, d_2, and d_3 scales, denoting

short-term and medium-term GARCH spillover effects from the Hang Seng Index spot to the CSI 300 Index spot. In terms of asymmetric spillover effects: (1) g_{11} is only significant at the d_4 scale, while g_{22} is significant at the d_1, d_2, and d_4 scales, showing stronger asymmetric impacts of the lagged terms on the Hang Seng Index spot compared to the CSI 300 Index spot; (2) g_{12} is significant at the d_1, d_2, and d_5 scales, suggesting asymmetric spillover effects from the CSI 300 Index spot to the Hang Seng Index spot at these scales; g_{21} is significant at the d_2 and d_3 scales, indicating medium-term asymmetric spillover effects from the Hang Seng Index spot to the CSI 300 Index spot.

From Table 5, it can be observed that in terms of mean spillover effects: (1) ϕ_{11} and ϕ_{22} are significant across all time scales, indicating a strong influence of the lagged terms on the returns of CSI 300 and Hang Seng Index futures; (2) ϕ_{12} is significant across all scales, denoting pervasive mean spillover effects from the CSI 300 Index futures to the Hang Seng Index futures; ϕ_{12} is significant across all scales except d_1, suggesting medium-term and long-term mean spillover effects from the Hang Seng Index futures to the CSI 300 Index futures. In terms of volatility spillover effects: (1) a_{11}, a_{22}, b_{11}, and b_{22} are significant across all time scales, indicating substantial impacts of their own lagged terms on the volatility of both indices' futures; (2) a_{12} is significant at the d_1, d_3, and d_5 scales, showing ARCH spillover effects from the CSI 300 Index futures to the Hang Seng Index futures across these scales; a_{21} is significant across all scales except d_3, suggesting mean spillover effects from the Hang Seng Index futures to the CSI 300 Index futures at short-term and long-term scales; (3) b_{12} is significant at the d_3 and d_5 scales, indicating GARCH spillover effects from the CSI 300 Index futures to the Hang Seng Index futures at these scales; b_{21} is significant at the d_1, d_3, and d_5 scales, denoting GARCH spillover effects from the Hang Seng Index futures to the CSI 300 Index futures across these scales. In terms of asymmetric spillover effects: (1) g_{11} and g_{22} are significant at the d_1, d_2, and d_4 scales, showing strong asymmetric impacts of the lagged terms on both indices' futures; (2) g_{12} is not significant across all scales, suggesting no asymmetric spillover effects from the CSI 300 Index futures to the Hang Seng Index futures; g_{21} is significant at the d_1, d_2, and d_4 scales, indicating asymmetric spillover effects from the Hang Seng Index futures to the CSI 300 Index futures at these scales.

Table 5. Estimation results of the VAR(1)-BEKK-AGARCH(1,1) model considering structural breaks (CSI 300 Index futures and Hang Seng Index futures)

	$\mathbf{d_1}$	$\mathbf{d_2}$	$\mathbf{d_3}$	$\mathbf{d_4}$	$\mathbf{d_5}$
Mean Equation					
φ_1	-0.0001	0.0002^{*}	-0.0001^{**}	-0.00002^{*}	0.00002^{***}
ϕ_{11}	-0.7234^{***}	0.3890^{***}	0.9129^{***}	1.0054^{***}	0.9874^{***}
ϕ_{12}	0.0335^{***}	0.0563^{***}	0.0295^{**}	0.0132^{***}	0.0104^{***}
φ_2	-0.0001	0.0001	-0.0001^{***}	0.00003^{***}	0.00001^{***}
ϕ_{21}	-0.0153	0.0256^{**}	-0.0456^{***}	0.0179^{***}	0.0077^{***}
ϕ_{22}	-0.6871^{***}	0.3431^{***}	1.0088^{***}	0.9563^{***}	1.0071^{***}
Variance Equation					
c_{11}	0.0083^{***}	0.0063^{***}	0.0040^{***}	0.0028^{***}	0.0017^{***}
c_{21}	0.0040^{***}	0.0022^{***}	0.0014^{***}	0.0009^{***}	0.0006^{***}
c_{22}	0.0062^{***}	0.0045^{***}	0.0029^{***}	0.0015^{***}	0.0011^{***}
a_{11}	0.8351^{***}	0.7971^{***}	1.3044^{***}	1.3059^{***}	1.3443^{***}
a_{12}	0.0428^{**}	0.0147	0.0510^{***}	-0.0049	-0.0032^{**}
a_{21}	0.0657^{**}	-0.1048^{***}	-0.0272	-0.0227^{***}	-0.0145^{***}
a_{22}	0.7657^{***}	0.7472^{***}	1.2063^{***}	1.3329^{***}	1.3091^{***}
b_{11}	0.6623^{***}	0.7014^{***}	0.3458^{***}	0.2709^{***}	0.2111^{***}
b_{12}	-0.0147	0.0045	0.0378^{***}	0.0044	0.0020^{*}
b_{21}	-0.0432^{*}	0.0369	-0.1696^{***}	-0.0276^{***}	0.0002
b_{22}	0.6584^{***}	0.6856^{***}	0.1223^{***}	0.2291^{***}	0.2052^{***}
g_{11}	-0.3256^{**}	-0.2917^{**}	0.0206	0.1178^{**}	0.0000
g_{12}	0.0191	0.0615	-0.0053	-0.0060	0.0000
g_{21}	-0.0342	-0.1141^{*}	-0.0425	-0.0346^{**}	0.0000
g_{22}	-0.3987^{***}	-0.4985^{***}	0.0310	0.0936^{*}	0.0000

Note: ***, **, and * denote significance levels at 1%, 5%, and 10%. 1 and 2 respectively represent the CSI 300 Index futures and the Hang Seng Index futures, respectively

From Table 6, it can be observed that in terms of mean spillover effects: (1) ϕ_{11} and ϕ_{22} are significant across all time scales, indicating a substantial impact of their own lagged terms on the returns of both spot and futures in the CSI 300 Index; (2) ϕ_{12} is significant at all scales except d1, suggesting the presence of mean spillover effects from the spot to the futures of this index at medium to long-term scales; ϕ_{21} is significant across all scales, indicating mean spillover effects from the futures to the spot of this index at all time scales. Concerning volatility spillover

effects: (1) a_{11}, a_{22}, b_{11}, and b_{22} are significant across all time scales, denoting a substantial impact of their own lagged terms on the volatility of both spot and futures in the CSI 300 Index. (2) a_{12}, a_{21}, b_{12}, and b_{21} are significant at scales d_2, d_3, and d_5, suggesting bidirectional ARCH and GARCH spillover effects between the spot and futures of this index at medium to long-term scales. Regarding asymmetric spillover effects: (1) g_{11} and g_{22} are significant at all scales except d_2, indicating strong asymmetric impacts of their own lagged terms on both spot and futures in the CSI 300 Index; (2) g_{12} and g_{21} are significant at scales d_1, d_3, and d_5, suggesting bidirectional asymmetric spillover effects between the spot and futures of this index at these scales.

Table 6. Estimation results of the VAR (1)-BEKK-AGARCH (1,1) model considering structural breaks (CSI 300 Index spot and futures)

	$\mathbf{d_1}$	$\mathbf{d_2}$	$\mathbf{d_3}$	$\mathbf{d_4}$	$\mathbf{d_5}$
Mean Equation					
φ_1	0.0000	0.0000	-0.00004^{**}	0.0000	0.00002^{***}
ϕ_{11}	-0.6484^{***}	0.1182^{***}	0.7526^{***}	0.8929^{***}	1.0562^{***}
ϕ_{12}	-0.0358	0.2557^{***}	0.0785^{***}	0.0617^{***}	-0.0438^{***}
φ_2	0.0000	0.0000	-0.00004^{**}	0.0000	0.00002^{***}
ϕ_{21}	0.0917^{***}	-0.2146^{***}	-0.0849^{***}	-0.0660^{***}	0.1123^{***}
ϕ_{22}	-0.7771^{***}	0.5814^{***}	0.9202^{***}	1.0246^{***}	0.9014^{***}
Variance Equation					
c_{11}	0.0036^{***}	0.0016^{***}	0.0007^{***}	0.0001^{***}	-0.00003^{***}
c_{21}	0.0031^{***}	0.0016^{***}	0.0006^{***}	0.0001^{***}	-0.00003^{***}
c_{22}	-0.0007^{***}	0.0003^{***}	-0.0001^{***}	-0.00002^{***}	0.000002^{***}
a_{11}	0.7739^{***}	1.4142^{***}	1.4443^{***}	1.4978^{***}	1.3837^{***}
a_{12}	-0.1077	0.6210^{***}	0.1965^{***}	0.0217	0.0427^{***}
a_{21}	0.0187	-0.6095^{***}	-0.1868^{***}	-0.0336	-0.0412^{***}
a_{22}	0.9239^{***}	0.2307^{***}	1.0607^{***}	1.4405^{***}	1.3003^{***}
b_{11}	0.6651^{***}	0.1122^{**}	0.5348^{***}	0.4357^{***}	0.5842^{***}
b_{12}	0.0529	0.6144^{***}	-0.0488^{**}	-0.0115	0.0108^{***}
b_{21}	0.0250	0.5621^{***}	0.0317	0.0017	0.0039^{***}
b_{22}	0.6363^{***}	1.2414^{***}	0.6141^{***}	0.4475^{***}	0.5989^{***}
g_{11}	-0.5888^{***}	0.2118	0.1760^{***}	-0.2019^{***}	0.1266^{***}
g_{12}	-0.4102^{***}	-0.0217	0.1514^{***}	0.0529	0.0749^{***}
g_{21}	0.6866^{***}	-0.0760	-0.1747^{***}	-0.0225	0.0866^{***}
g_{22}	0.5756^{***}	0.1814	-0.1632^{***}	-0.2781^{***}	0.0360^{***}

Note: ***, **, and * denote significance levels at 1%, 5%, and 10%. 1 and 2 respectively represent the CSI 300 Index spot and futures, respectively

From Table 7, it can be observed that in terms of mean spillover effects: (1) ϕ_{11} and ϕ_{22} are significant across all time scales, indicating a substantial impact of their own lagged terms on the returns of both spot and futures in the Hang Seng Index; (2) ϕ_{12} and ϕ_{21} are significant at all scales except d_4, suggesting bidirectional mean spillover effects between the spot and futures of this index at short to medium-term scales. Concerning volatility spillover effects: (1) a_{11}, a_{22}, b_{11}, and b_{22} are significant across all time scales, denoting a substantial impact of their own lagged terms on the volatility of both spot and futures in the Hang Seng Index. (2) a_{12} is significant at all scales except d_4, indicating ARCH spillover effects from the spot to the futures of this index at short to medium-term scales; a_{21} is significant at scales d_1, d_2, and d_3, suggesting ARCH spillover effects from the futures to the spot of this index at short to medium-term scales. (3) b_{12} and b_{21} are significant across all scales, suggesting bidirectional GARCH spillover effects between the spot and futures of this index at all time scales. Regarding asymmetric spillover effects: (1) g_{11} and g_{22} are significant at all scales except d_2, indicating strong asymmetric impacts of their own lagged terms on both spot and futures in the Hang Seng Index; (2) g_{12} and g_{21} are significant at all scales except d_2, suggesting bidirectional asymmetric spillover effects between the spot and futures of this index at short and long-term scales.

A comprehensive summary of the mean, volatility, and asymmetric spillover effects between different markets across various time scales has been collated based on the parameter estimation results from Tables 4–7, and is presented in Table 8. It can be observed that there are differences in the spillover effects between the CSI 300 and Hang Seng Index spot and futures markets across different time scales. Specifically, (1) for markets of different indices, bidirectional mean spillover effects are present only at the long-term scale d_5 between the spot markets of the two indices; bidirectional mean spillover effects exist at medium to long-term scales except d1 between the futures markets of the two indices; unidirectional volatility spillover effects are prevalent at most scales between the spot and futures markets of the two indices; asymmetric spillover effects are present at all scales except d_4 between the spot

markets of the two indices; asymmetric spillover effects exist only at scales d_2 and d_5 between the futures markets of the two indices. (2) For markets of the same index, bidirectional mean and volatility spillover effects are present at all scales except d1 and d4 between the spot and futures markets of the same index; bidirectional asymmetric spillover effects are observed at all scales except d_2 and d_4. These findings indicate relatively stronger spillover effects in mean, volatility, and asymmetry between the spot and futures markets of the same index compared to markets of different indices. Building upon the study of risk spillover effects in the CSI 300 and Hang Seng Index spot and futures markets, further research is conducted on the hedging issues between spot and futures markets in this text.

Table 7. Estimation results of the VAR (1)-BEKK-AGARCH (1,1) model considering structural breaks (Hang Seng Index spot and futures)

	$\mathbf{d_1}$	$\mathbf{d_2}$	$\mathbf{d_3}$	$\mathbf{d_4}$	$\mathbf{d_5}$
Mean Equation					
φ_1	-0.00002^{***}	0.0000	0.0000	-0.00003^{***}	-0.00003^{***}
ϕ_{11}	-0.7626^{***}	0.2786^{***}	0.5693^{***}	0.9650^{***}	0.9946^{***}
ϕ_{12}	0.0620^{***}	0.1125^{***}	0.3020^{***}	-0.0124	0.0128^{***}
φ_2	-0.00003^{***}	0.0000	0.0000	-0.00003^{***}	0.0000^{***}
ϕ_{21}	-0.0192^{***}	-0.0466^{*}	-0.2546^{***}	0.0047	0.0187^{***}
ϕ_{22}	-0.6924^{***}	0.4098^{***}	1.1223^{***}	0.9453^{***}	0.9878^{***}
Variance Equation					
c_{11}	0.0021^{***}	0.0011^{***}	0.0004^{***}	0.0001^{***}	0.0015^{***}
c_{21}	0.0022^{***}	0.0012^{***}	0.0005^{***}	0.0001^{***}	0.0015^{***}
c_{22}	0.0007^{***}	0.0001	-0.00004^{***}	0.0000	0.0000
a_{11}	0.6314^{***}	1.4893^{***}	1.4938^{***}	1.4508^{***}	0.5642^{***}
a_{12}	-0.2161^{***}	0.7357^{***}	0.2512^{***}	-0.0091	0.0015^{***}
a_{21}	0.1644^{***}	-0.6997^{***}	-0.2159^{***}	0.0146	0.0001
a_{22}	0.9961^{***}	0.1013	1.0329^{***}	1.4788^{***}	0.5662^{***}
b_{11}	0.8392^{***}	-0.1422^{**}	0.5822^{***}	0.4564^{***}	0.8314^{***}
b_{12}	0.2035^{***}	-0.8749^{***}	0.0285^{***}	0.0170^{***}	-0.0104^{***}
b_{21}	-0.1451^{***}	0.8231^{***}	-0.0716^{***}	-0.0176^{***}	-0.0062^{***}
b_{22}	0.4953^{***}	1.5155^{***}	0.4811^{***}	0.4215^{***}	0.8359^{***}
g_{11}	0.3980^{***}	0.0229	0.4804^{***}	-0.1228^{***}	0.3673^{***}
g_{12}	0.3095^{***}	0.0773	0.4568^{***}	-0.0249^{**}	-0.0871^{***}
g_{21}	-0.5673^{***}	0.1063	-0.3311^{**}	0.0089^{*}	0.1041^{***}
g_{22}	-0.5680^{***}	0.0384	-0.3120^{***}	-0.0872^{*}	0.5588^{***}

Note: ***, **, and * respectively denote significance levels at 1%, 5%, and 10%. 1 and 2 respectively represent Hang Seng Index spot and futures

Table 8. Summary of spillover effects between markets

	$\mathbf{d_1}$	$\mathbf{d_2}$	$\mathbf{d_3}$	$\mathbf{d_4}$	$\mathbf{d_5}$
Mean Spillover Effect					
Shanghai-Shenzhen Spot - Hang Seng Spot	U($\leftarrow$)	U($\rightarrow$)	U($\leftarrow$)	U($\leftarrow$)	B($\leftrightarrow$)
Shanghai-Shenzhen Futures - Hang Seng Futures	U($\rightarrow$)	B($\leftrightarrow$)	B($\leftrightarrow$)	B($\leftrightarrow$)	B($\leftrightarrow$)
Shanghai-Shenzhen Spot - Shanghai-Shenzhen Futures	U($\leftarrow$)	B($\leftrightarrow$)	B($\leftrightarrow$)	B($\leftrightarrow$)	B($\leftrightarrow$)
e Hang Seng Spot - Hang Seng Futures	B($\leftrightarrow$)	B($\leftrightarrow$)	B($\leftrightarrow$)	NO	B($\leftrightarrow$)
Volatility Spillover Effect (ARCH and GARCH Spillover Effects)					
Shanghai-Shenzhen Spot - Hang Seng Spot	U($\leftarrow$)	U($\leftarrow$)	B($\leftrightarrow$)	U($\rightarrow$)	B($\leftrightarrow$)
Shanghai-Shenzhen Futures - Hang Seng Futures	B($\leftrightarrow$)	U($\leftarrow$)	B($\leftrightarrow$)	U($\leftarrow$)	B($\leftrightarrow$)
Shanghai-Shenzhen Spot - Shanghai-Shenzhen Futures	NO	B($\leftrightarrow$)	B($\leftrightarrow$)	NO	B($\leftrightarrow$)
Hang Seng Spot - Hang Seng Futures	B($\leftrightarrow$)	B($\leftrightarrow$)	B($\leftrightarrow$)	B($\leftrightarrow$)	B($\leftrightarrow$)
Asymmetric Spillover Effect					
Shanghai-Shenzhen Spot - Hang Seng Spot	U($\rightarrow$)	B($\leftrightarrow$)	U($\leftarrow$)	NO	U($\rightarrow$)
Shanghai-Shenzhen Futures - Hang Seng Futures	NO	U($\leftarrow$)	NO	U($\leftarrow$)	NO
Shanghai-Shenzhen Spot - Shanghai-Shenzhen Futures	B($\leftrightarrow$)	NO	B($\leftrightarrow$)	NO	B($\leftrightarrow$)
Hang Seng Spot - Hang Seng Futures	B($\leftrightarrow$)	NO	B($\leftrightarrow$)	U($\rightarrow$)	B($\leftrightarrow$)

Note: "U" indicates that the spillover effect is unidirectional, "B" indicates that the spillover effect is bidirectional, and the direction of the spillover is shown inside the parentheses. "NO" signifies that there is no spillover effect between the two markets at that scale

3.4 Dynamic Hedging Results

Based on Eq. (9), the optimal dynamic hedge ratios and hedging performance between the CSI 300 Index spot and futures, as well as between the Hang Seng Index spot and futures, were calculated under the VAR-BEKK-AGARCH model considering structural breaks. These results were then compared with the models that do not consider structural breaks, as well as with the static hedging results obtained using Ordinary Least Squares (OLS) method, as presented in Table 9.

Table 9. Estimation results for hedge ratios and hedging effectiveness

	CSI 300 Index					**Hang Seng Index**				
	d_1	d_2	d_3	d_4	d_5	d_1	d_2	d_3	d_4	d_5
Static Hedging										
Ratio	0.9132	0.8094	0.9824	0.8492	0.9238	0.9974	1.1260	0.8682	0.9992	1.3358
HE	0.8480	0.8697	0.9291	0.9424	0.9890	0.9253	0.9619	0.9497	0.9904	0.9948
Dynamic Hedging (Not Considering Structural Breaks)										
Ratio Mean	0.9316	0.9501	0.9700	0.9682	0.9289	0.9167	0.9442	0.9759	0.9682	0.9863
Ratio Variance	0.0477	0.0396	0.1092	0.0656	0.1056	0.0166	0.0131	0.0439	0.0656	0.0245
HE	0.8690	0.8982	0.9273	0.9555	0.9630	0.9234	0.9467	0.9492	0.9955	0.9841
Dynamic Hedging (Considering Structural Breaks)										
Ratio Mean	0.9245	0.9496	0.9705	0.9349	0.9181	0.9220	0.9394	0.9746	0.9672	0.9955
Ratio Variance	0.0445	0.0398	0.1019	0.2116	0.0459	0.0184	0.0150	0.0442	0.0677	0.0105
HE	0.8700	0.8997	0.9298	0.9575	0.9813	0.9265	0.9744	0.9597	0.9958	0.9903

Observations can be made as follows: (1) At the same time scale, compared to the CSI 300 Index, the Hang Seng Index demonstrates a smaller volatility in hedge ratios. Moreover, the HE values of the Hang Seng Index hedging portfolio consistently surpass those of the CSI 300 Index at corresponding levels; (2) With an increase in the time scale, a gradual augmentation is noted in the HE values of the CSI 300 Index hedging portfolio, indicating an enhancement in hedging effectiveness. In contrast, the HE values of the Hang Seng Index hedging portfolio exhibit irregular fluctuations with the change in time scale; (3) At each scale, the HE values of the dynamic hedging portfolio considering structural breaks are consistently higher than those not accounting for structural breaks. This suggests that the dynamic hedging portfolio, which takes structural breaks into account, outperforms the portfolio that neglects structural breaks. (4) Except for at d_5 scale, the HE values of the dynamic hedging portfolio considering structural breaks exceed those of the static hedging portfolio. This denotes a superiority of the dynamic hedging portfolio over the static hedging counterpart in the short to medium term scales.

3.5 Wavelet Coherence and Phase Difference Analyses

Figures 6 and 7 respectively illustrate the wavelet coherence and phase difference between the CSI 300 Index spot and futures and the Hang Seng Index spot and futures. The color bar to the right of the figures indicates the level of coherence, with blue representing low coherence and yellow representing high coherence. The vertical axis denotes frequency, while the horizontal axis represents time. Arrows indicate wavelet phase difference, illustrating the lead-lag relationship between index fluctuations in time and frequency domains. It is observed that: (1) There is a prevalence of yellow areas at lower frequencies (long-term scales), indicating a significant correlation between the two markets. (2) Throughout the entire sample period, an apparent increase in yellow areas is noted post-2017, signifying an augmented correlation between the two markets since the initiation of the "Shanghai-Hongkong Stock Connect" on December 5, 2016. This initiative has fostered a closer connection between the Shanghai/Shenzhen and Hong Kong markets post-2017. (3) Predominantly, arrows point horizontally to the right, indicating that the CSI 300 Index and Hang Seng Index generally move in the same direction. Some arrows point diagonally from the top left to the bottom right and from the bottom left to the top right, with angles within the range of $[-2/\pi, 2/\pi]$. This implies a small phase difference between the CSI 300 Index and the Hang Seng Index, devoid of a fixed lead-lag relationship. This connotes a tightly linked and mutually influencing relationship between the two markets.

Figures 8 and 9 respectively present the wavelet coherence and phase difference between the CSI 300 Index spot and futures, and the Hang Seng Index spot and futures. It is observed that: (1) The correlation between the two indices' spot and futures varies across different time scales. At higher frequencies (short-term scales), the correlation between spot and futures is relatively low. Specifically, on the d_1–d_4 scales, the correlation between the CSI 300 Index spot and futures demonstrates volatility, particularly from June 2014 to June 2017, where fluctuations were exceptionally intense, and arrows were chaotically arranged. This period was marked by the stock market crash in China, leading to instability in both the CSI 300 Index spot and futures markets, with a slight reduction in their correlation. The correlation between the Hang Seng Index spot and futures experienced minor fluctuations on the d_1

scale. At lower frequencies (medium to long-term scales), high correlation is observed between the spot and futures of both indices, with the correlation approaching 1 as the time scale increases. (2) Nearly all arrows point to the right, indicating that the spot and futures of the two indices generally move in sync, with a small phase difference, and no apparent lead-lag relationship. This further verifies that the spot and futures of the CSI 300 and Hang Seng Index serve as effective hedging tools.

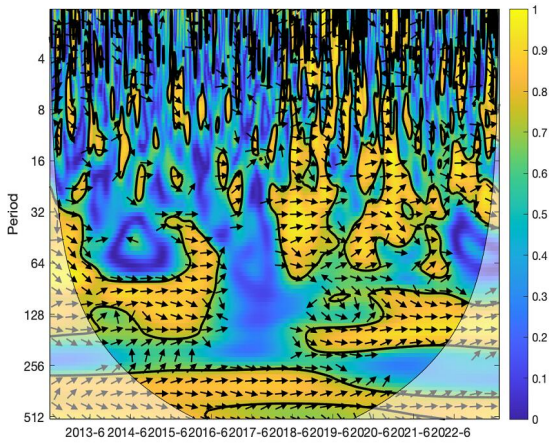

Figure 6. Wavelet coherence and phase difference between CSI 300 spot and Hang Seng spot

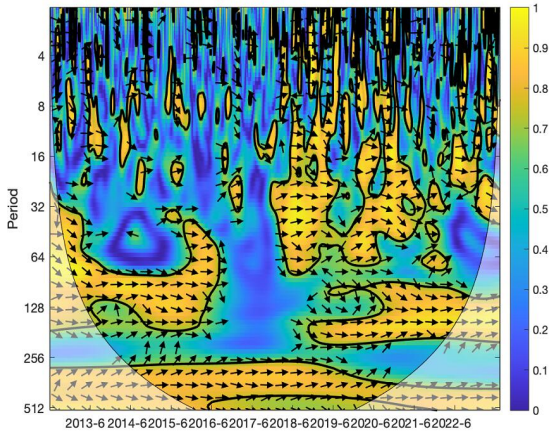

Figure 7. Wavelet coherence and phase difference between CSI 300 futures and Hang Seng futures

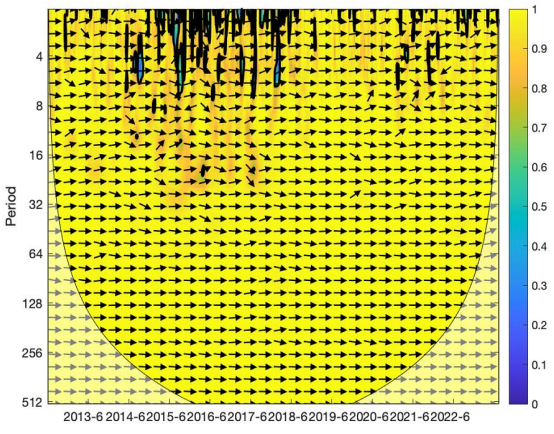

Figure 8. Wavelet coherence and phase difference between spot and futures of the CSI 300 Index

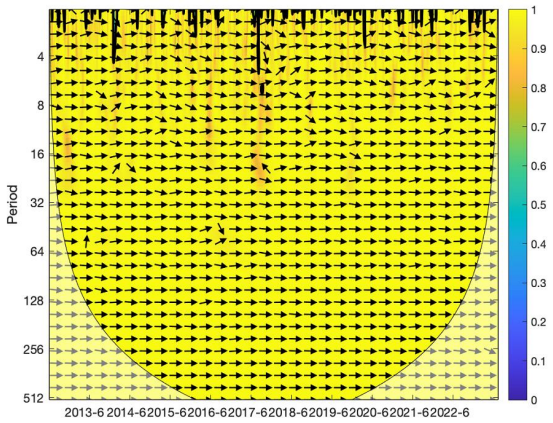

Figure 9. Wavelet coherence and phase difference between spot and futures of the Hang Seng Index

4 Conclusions

In order to investigate the multi-scale risk spillover and dynamic hedging issues in the Chinese stock market, considering structural breaks, this study employs the maximal overlap discrete wavelet transform method to decompose the spot and futures returns of the CSI 300 and Hang Seng Index into short-term, medium-term, and long-term time scales. Additionally, an asymmetric VAR-BEKK-AGARCH model, accounting for the structural breaks in return volatility, has been constructed to explore the mean spillover, volatility spillover, and asymmetric spillover effects between the CSI 300 and Hang Seng Index, as well as between the spot and futures markets of the two indices at different time scales. Furthermore, dynamic hedging portfolios of spot and futures for each index have been constructed to analyze the hedging performance across different time scales. Lastly, wavelet coherence and phase difference analyses have been utilized to validate the research findings.

The results have indicated that:

(1) The VAR-BEKK-AGARCH model, which takes into account structural breaks, is found to be more applicable to the stock market data of China than the model without consideration of structural breaks.

(2) At different time scales, the mean spillover, volatility spillover effects, and asymmetric effects between the spot and futures markets of the CSI 300 and Hang Seng Index vary. Compared to different index markets, the risk spillover effects between the spot and futures markets of the same index are relatively stronger.

(3) In terms of hedging performance, the dynamic hedging portfolio considering structural breaks outperforms the portfolio without consideration of structural breaks. Moreover, at short and medium-term scales, the dynamic hedging portfolio considering structural breaks is superior to the static hedging portfolio.

(4) Analysis via wavelet coherence and phase difference suggests that the CSI 300 Index, Hang Seng Index, and the spot and futures of each index generally move in the same direction, with a small phase difference between the two indices, lacking a fixed lead-lag relationship. Additionally, a stronger correlation between the markets is observed at longer time scales. This further substantiates that the spot and futures of the CSI 300 and Hang Seng Index serve as effective tools for hedging.

Funding

This work was supported by the Social Science Foundation in Hebei Province of China (HB22YJ035).

Data Availability

The data used to support the research findings are available from the corresponding author upon request.

Conflicts of Interest

The authors declare no conflict of interest.

References

[1] X. Zhou, J. Zhang, and Z. Zhang, "How does news flow affect cross-market volatility spillovers? Evidence from China's stock index futures and spot markets," *Int. Rev. Econ. Finance*, vol. 73, no. 73, pp. 196–213, 2021. https://doi.org/10.1016/j.iref.2021.01.003

[2] K. Gkillas, C. Konstantatos, C. Floros, and A. Tsagkanos, "Realized volatility spillovers between US spot and futures during ECB news: Evidence from the European sovereign debt crisis," *Int. Rev. Financial Anal.*, vol. 74, no. 74, p. 101706, 2021. https://doi.org/10.1016/j.irfa.2021.101706

[3] S. Corbet, Y. Hou, Y. Hu, and L. Oxley, "The influence of the COVID-19 pandemic on the hedging functionality of Chinese financial markets," *Res. Int. Bus. Finance*, vol. 59, no. 59, p. 101510, 2022. https://doi.org/10.1016/j.ribaf.2021.101510

[4] I. Yousaf, M. Beljid, A. Chaibi, and A. Ajlouni, "Do volatility spillover and hedging among GCC stock markets and global factors vary from normal to turbulent periods? Evidence from the global financial crisis and Covid-19 pandemic crisis," *Pac. Basin Finance J.*, vol. 2022, no. 73, p. 101764, 2022. https://doi.org/10.1016/j.pacfin.2022.101764

[5] R. MacDonald, V. Sogiakas, and A. Tsopanakis, "Volatility co-movements and spillover effects within the Eurozone economies: A multivariate GARCH approach using the financial stress index," *J. Int. Financial Markets Institutions Money*, vol. 52, no. 52, pp. 17–36, 2018. https://doi.org/10.1016/j.intfin.2017.09.003

[6] C. Wang and Y. S. Wei, "Simulation of financial risk spillover effect based on ARMA-GARCH and fuzzy calculation model," *J. Intelli. Fuzzy Syst.*, vol. 40, no. 4, pp. 6555–6566, 2021. https://doi.org/10.3233/JIFS-189493

[7] X. Tan, X. Wang, S. Ma, Z. Wang, Y. Zhao, and L. Xiang, "Covid-19 shock and the time-varying volatility spillovers among the energy and precious metals markets: Evidence from a DCC-GARCH-CONNECTEDNESS approach," *Front. Publ. Health*, vol. 10, no. 10, p. 906969, 2022. https://doi.org/10.3389/fpubh.2022.906969

[8] Z. Pan, Y. Wang, L. Liu, and Q. Wang, "Improving volatility prediction and option valuation using VIX information: A volatility spillover GARCH model," *J. Futures Markets*, vol. 39, no. 6, pp. 744–776, 2019.

[9] K. Malik, S. Sharma, and M. Kaur, "Measuring contagion during COVID-19 through volatility spillovers of BRIC countries using diagonal BEKK approach," *J. Econ. Stud.*, vol. 49, no. 2, pp. 227–242, 2021. https://doi.org/10.1108/jes-05-2020-0246

[10] G. Dhaene, P. Sercu, and J. B. Wu, "Volatility spillovers: A sparse multivariate GARCH approach with an application to commodity markets," *J. Futures Markets*, vol. 42, no. 5, pp. 868–887, 2022. https://doi.org/10.1002/fut.22312

[11] L. Yu, R. Zha, D. Stafylas, K. He, and J. Liu, "Dependences and volatility spillovers between the oil and stock markets: New evidence from the copula and VAR-BEKK-GARCH models," *Int. Rev. Financial Anal.*, vol. 68, no. 68, p. 101280, 2020. https://doi.org/10.1016/j.irfa.2018.11.007

[12] F. Malik, "Volatility spillover between exchange rate and stock returns under volatility shifts," *Q. Rev. Econ. Finance*, vol. 80, no. 80, pp. 605–613, 2021. https://doi.org/10.1016/j.qref.2021.04.011

[13] F. Malik, "Volatility spillover among sector equity returns under structural breaks," *Rev. Quant. Finance Acc.*, vol. 58, no. 3, pp. 1063–1080, 2021. https://doi.org/10.1007/s11156-021-01018-8

[14] W. Mensi, K. Al-Yahyaee, and S. Kang, "Time-varying volatility spillovers between stock and precious metal markets with portfolio implications," *Resour. Policy*, vol. 2017, no. 53, pp. 88–102, 2017. https://doi.org/10.1016/j.resourpol.2017.06.001

[15] S. Sarwar, R. Khalfaoui, R. Waheed, and H. G. Dastgerdi, "Volatility spillovers and hedging: Evidence from Asian oil-importing countries," *Resour. Policy*, vol. 61, no. 61, pp. 479–488, 2019. https://doi.org/10.1016/j.resourpol.2018.04.010

[16] F. Wen, J. Cao, Z. Liu, and X. Wang, "Dynamic volatility spillovers and investment strategies between the Chinese stock market and commodity markets," *Int. Rev. Financial Anal.*, vol. 76, no. 76, p. 101772, 2021. https://doi.org/10.1016/j.irfa.2021.101772

[17] M. Arfaoui, W. Chkili, and A. B. Rejeb, "Asymmetric and dynamic links in GCC Sukuk-stocks: Implications for portfolio management before and during the COVID-19 pandemic," *J. Econ. Asymmetries*, vol. 25, no. 25, p. e00244, 2022. https://doi.org/10.1016/j.jeca.2022.e00244

[18] J. Cui, M. Goh, B. Li, and H. Zou, "Dynamic dependence and risk connectedness among oil and stock markets: New evidence from time-frequency domain perspectives," *Energy*, vol. 2021, no. 216, p. 119302, 2021. https://doi.org/10.1016/j.energy.2020.119302

[19] J. Li, R. Liu, Y. Yao, and Q. Xie, "Time-frequency volatility spillovers across the international crude oil market and Chinese major energy futures markets: Evidence from COVID-19," *Resour. Policy*, vol. 77, no. 77, p. 102646, 2022. https://doi.org/10.1016/j.resourpol.2022.102646

[20] S. Qureshi, F. Qureshi, A. B. Soomro, F. H. Chandio, S. S. Shah, and I. U. Rehman, "Exchange rate risk and sectoral returns: A wavelet-based MRA-EDCC GARCH analysis," *Commun. Stat. Theor. Methods*, vol. 51, no. 7, pp. 2154–2182, 2020. https://doi.org/10.1080/03610926.2020.1772304

[21] D. Zivkov, J. Duraskovic, and M. GajicGlamoclija, "Multiscale downside risk interdependence between the major agricultural commodities," *Agribusiness*, vol. 38, no. 4, pp. 990–1011, 2022. https://doi.org/10.1002/agr.21749

[22] S. Gürbüz and A. Şahbaz, "Investigating the volatility spillover effect between derivative markets and spot markets via the wavelets: The case of Borsa istanbul," *Borsa Istanbul Rev.*, vol. 22, no. 2, pp. 321–331, 2022.

https://doi.org/10.1016/j.bir.2021.05.006

[23] O. Belhassine and C. Karamti, "Volatility spillovers and hedging effectiveness between oil and stock markets: Evidence from a wavelet-based and structural breaks analysis," *Energy Econ.*, vol. 102, no. 102, p. 105513, 2021. https://doi.org/10.1016/j.eneco.2021.105513

[24] B. Zheng, Y. W. Zhang, F. Qu, Y. Geng, and H. Yu, "Do rare earths drive volatility spillover in crude oil, renewable energy, and high-technology markets? — A wavelet-based BEKK- GARCH-X approach," *Energy*, vol. 251, p. 123951, 2022. https://doi.org/10.1016/j.energy.2022.123951

[25] I. Fasanya, O. Oyewole, and O. Adekoya, "Oil price and stock market behaviour in GCC countries: Do asymmetries and structural breaks matter?" *Energy Strategy Rev.*, vol. 2021, no. 36, p. 100682, 2021. https://doi.org/10.1016/j.esr.2021.100682

[26] V. Aragó-Manzana and M. Á. Fernández-Izquierdo, "Influence of structural changes in transmission of information between stock markets: A European empirical study," *J. Multinational Financial Manage.*, vol. 17, no. 2, pp. 112–124, 2007. https://doi.org/10.1016/j.mulfin.2006.05.002

[27] L. Zhao and F. Wen, "Risk-return relationship and structural breaks: Evidence from China carbon market," *Int. Rev. Econ. Finance*, vol. 77, no. 77, pp. 481–492, 2022. https://doi.org/10.1016/j.iref.2021.10.019

[28] Q. Chen and X. Weng, "Information Flows Between the US and China's Agricultural Commodity Futures Markets—Based on VAR–BEKK–Skew-t Model," *Emerg. Markets Finance Trade*, vol. 54, no. 1, pp. 71–87, 2017. https://doi.org/10.1080/1540496x.2016.1230492

[29] P. Kapler, "An application of continuous wavelet transform and wavelet coherence for residential power consumer load profiles analysis," *Bull. Pol. Acad. Sci.*, vol. 69, no. 9, pp. 1–8, 2023. https://doi.org/10.24425/bpasts.2020.136216

[30] H. Zhu, D. Yu, L. Hau, H. Wu, and F. Ye, "Time-frequency effect of crude oil and exchange rates on stock markets in BRICS countries: Evidence from wavelet quantile regression analysis," *North Am. J. Econ. Finance*, vol. 61, no. 61, p. 101708, 2022. https://doi.org/10.1016/j.najef.2022.101708

Appendix

Table A1. Results of structural break detection

	$\mathbf{d_1}$	$\mathbf{d_2}$	$\mathbf{d_3}$	$\mathbf{d_4}$	$\mathbf{d_5}$
CSI 300 Index Spot	2014-05-14	2014-05-26		2014-01-03	2014-01-10
	2015-05-14	2015-06-03		2014-09-19	2014-09-30
	2016-05-06	2016-06-07		2015-12-07	2016-01-15
	2017-01-26	2017-03-06		2017-02-23	2017-04-13
	2018-01-24	2018-12-07		2018-01-17	2018-03-23
	2018-10-12	2020-03-24		2018-11-16	2019-06-21
	2020-01-16	2021-06-25		2019-06-28	2020-05-29
	2021-05-28			2020-07-24	2021-04-30
				2021-08-20	2022-01-11
CSI 300 Index Futures	2014-01-27	2014-05-30	2014-01-10	2014-01-03	2014-01-10
	2014-10-31	2015-06-16	2014-09-30	2014-09-19	2014-09-30
	2016-02-29	2016-06-24	2015-12-24	2015-12-07	2016-01-15
	2017-05-05	2017-03-24	2017-03-21	2017-02-23	2017-04-13
	2018-03-28	2018-03-29	2018-02-12	2018-01-17	2018-03-23
	2019-02-01	2019-01-02	2018-12-14	2018-11-16	2019-06-21
	2019-09-30	2020-04-24	2019-07-19	2019-06-28	2020-05-29
	2020-08-21	2021-07-09	2020-08-07	2020-07-24	2021-04-30
	2021-04-14		2021-08-27		2022-01-11
Hang Seng Index Spot	2014-05-14	2014-05-26		2014-01-03	2014-01-10
	2015-05-14	2015-06-03		2014-09-19	2014-09-30
	2016-05-06	2016-06-07		2015-12-07	2016-01-15
	2017-01-26	2017-03-06		2017-02-23	2017-04-13
	2018-01-24	2018-03-09		2018-01-17	2018-03-23
	2018-10-12	2018-12-07		2018-11-16	2019-06-21
	2020-01-16	2020-03-24		2019-06-28	2020-05-29
	2021-05-28	2021-06-25		2020-07-24	2021-04-30
				2021-08-20	2022-01-11
Hang Seng Index Futures	2013-10-11	2013-10-25	2014-01-10	2014-01-03	2014-01-10
	2014-05-14	2014-05-30	2014-09-30	2014-09-19	2014-09-30
	2015-05-14	2015-06-16	2015-12-24	2015-12-07	2016-01-15
	2016-05-06	2016-06-24	2017-03-21	2017-02-23	2017-04-13
	2017-01-26	2017-03-24	2018-02-12	2018-01-17	2018-03-23
	2018-10-12	2018-03-29	2020-08-07	2018-11-16	2019-06-21
	2019-07-05	2019-01-02		2019-06-28	2020-05-29
	2020-01-16	2019-09-30		2020-07-24	2021-04-30
	2020-10-23	2020-04-24		2021-08-20	2022-01-11
	2021-05-28	2021-01-04			

Note: The dates of breaks were estimated using the modified ICSS algorithm applied to the residuals of the VAR (1)-BEKK-AGARCH model